

1

Study of Λ_b^0 and Ξ_b^0 Decays to $\Lambda h^+ h'^-$ and Evidence for CP Violation in $\Lambda_b^0 \rightarrow \Lambda K^+ K^-$ Decays

2

3

R. Aaij *et al.*^{*}

4

5

(LHCb Collaboration)

6

(Received 23 November 2024; accepted 22 January 2025)

7

8

9

10

11

12

13

14

15

A study of Λ_b^0 and Ξ_b^0 decays to $\Lambda h^+ h'^-$ ($h'^\ell = \pi, K$) is performed using pp collision data collected by the LHCb experiment during LHC Runs 1–2, corresponding to an integrated luminosity of 9 fb^{-1} . The branching fractions for these decays are measured using the $\Lambda_b^0 \rightarrow \Lambda_c^+(\rightarrow \Lambda\pi^+)\pi^-$ decay as a control channel. The decays $\Lambda_b^0 \rightarrow \Lambda\pi^+\pi^-$ and $\Xi_b^0 \rightarrow \Lambda K^-\pi^+$ are observed for the first time. For decay modes with sufficient signal yields, CP asymmetries are measured in the full and localized regions of the final-state phase space. Evidence is found for CP violation in the $\Lambda_b^0 \rightarrow \Lambda K^+K^-$ decay, interpreted as originating primarily from an asymmetric $\Lambda_b^0 \rightarrow N^{*+}K^-$ decay amplitude. The measured CP asymmetries for other decays are compatible with zero.

16

DOI:

In the standard model (SM) of particle physics, symmetry breaking under the combined charge-conjugation and parity transformations (CP violation) originates from a complex phase within the Cabibbo-Kobayashi-Maskawa (CKM) matrix [1]. To date, all observed CP violation phenomena align with the CKM mechanism. However, the amount of CP violation in the SM is insufficient to explain the observed matter–antimatter imbalance in the Universe [2], motivating further study of CP violation and searches for possible new sources beyond the SM contributions.

While the breaking of CP symmetry has been established and extensively studied in K , B , and D meson decays, it has never been observed in any baryon decay. The BESIII experiment has conducted comprehensive searches for CP violation in light hyperon decays, including studies of decay rates and parameters, finding no evidence for CP violation [3]. Searches for CP violation have been pursued by LHCb in bottom-baryon decays, including $\Lambda_b^0 \rightarrow K_S^0 p\pi^-$ [4] $\Lambda_b^0 \rightarrow J/\psi p\pi^-$ [5] $\Lambda_b^0 \rightarrow ph^-h'^+h''^+$ [6–10], $\Lambda_b^0 \rightarrow \Lambda K^+K^-$, $\Lambda_b^0 \rightarrow \Lambda K^+\pi^-$ [11], $\Lambda_b^0 \rightarrow pK^-\mu^+\mu^-$ [12], $\Lambda_b^0 \rightarrow ph^-$ [13], $\Xi_b^- \rightarrow pK^-K^-$ [14], $\Lambda_b^0 \rightarrow \Lambda\gamma$ [15], $\Lambda_b^0 \rightarrow \Lambda\phi$ [16], and charm-baryon decays such as $\Lambda_c^+ \rightarrow ph^+h^-$ [17] and $\Xi_c^+ \rightarrow pK^-\pi^+$ [18], where $h, h', h'' = \pi$ or K throughout this Letter (the inclusion of charge-conjugated processes is implied

throughout the Letter if not specified.). These measurements are statistically limited and rely mostly on data collected during LHC Run 1 (2011–2012). Further investigation of CP violation in baryon decays may shed new light on the dynamics of weak decays in the baryon sector and provide a better picture of CP violation originating from quark transitions.

In three-body charmless B -meson decays, $B \rightarrow h^+h'^-h''^+$, large CP violation up to 75% is observed in localized regions of phase space, for example, in the low K^+K^- , low $\pi^+\pi^-$ and high $\pi^+\pi^-$ mass regions [19–21]. These results suggest that resonance interactions and $\pi^+\pi^- \leftrightarrow K^+K^-$ S-wave rescattering play an important role in the generation of strong phases needed for direct CP violation, and motivate further studies of Λ_b^0 and Ξ_b^0 decays to $\Lambda h^+h'^-$ final states, which are governed by similar dynamics in the SM.

Quasi-two-body charmless Λ_b^0 decays, $\Lambda_b^0 \rightarrow \Lambda\omega/\Lambda\phi/\Lambda\rho$, have been studied with the QCD factorization approach and their CP violation is predicted to be in the range 0% to 4% with branching fractions at the level of 10^{-7} [22–25]. The generalized factorization approach (GFA), considering part of the nonfactorizable sources by introducing an effective color number N_c , gives similar CP asymmetry predictions and the branching fractions are predicted to be approximately 10^{-6} [26,27]. For the $\Lambda_b^0 \rightarrow N^{*+}\pi^-$ decay, the CP asymmetry is predicted to be in the range from -4% to 6% [28]. In a previous LHCb study, the $\Lambda_b^0 \rightarrow \Lambda K^+K^-$ and $\Lambda_b^0 \rightarrow \Lambda K^+\pi^-$ decays were observed with the Run 1 sample [11], where the first evidence for $\Lambda_b^0 \rightarrow \Lambda\pi^+\pi^-$ was established and the CP asymmetries for these decays were found to be compatible with zero. Further higher-precision measurements of CP asymmetries and branching fractions of Λ_b^0 and Ξ_b^0 decays to $\Lambda h^+h'^-$ final states offer stringent

^{*}Full author list given at the end of the Letter.

75 tests of these models and provide a foundation to study other
 76 quasi-two-body decays that have not been considered before.

77 This Letter reports the measurements of branching
 78 fractions and CP violation parameters for charmless decays
 79 of Λ_b^0 and Ξ_b^0 baryons into the final states $\Lambda K^\pm \pi^\mp$, $\Lambda K^+ K^-$,
 80 and $\Lambda \pi^+ \pi^-$, among which the suppressed modes
 81 $\Lambda_b^0 \rightarrow \Lambda K^- \pi^+$ and $\Xi_b^0 \rightarrow \Lambda K^+ \pi^-$ are not considered. The
 82 study is performed based on proton-proton (pp) collision
 83 data collected with the LHCb detector during LHC Runs 1–
 84 2 (2011–2018) at center-of-mass energies of 7, 8, and
 85 13 TeV and corresponding to an integrated luminosity of
 86 9 fb^{-1} . The $\Lambda_b^0 \rightarrow \Lambda_c^+ (\rightarrow \Lambda \pi^+) \pi^-$ decay is used as control
 87 channel for both the branching fraction and CP -violation
 88 measurements to reduce systematic uncertainties.

89 The LHCb detector is a single-arm forward spectrometer
 90 covering the pseudorapidity range $2 < \eta < 5$, described in
 91 detail in Refs. [29,30]. It is designed specifically for the
 92 study of particles containing b or c quarks. Of particular
 93 relevance for this analysis is the tracking system, comprising
 94 silicon-strip stations upstream and straw drift tube stations
 95 downstream of a 4 Tm dipole magnet [31,32], and the ring-
 96 imaging Cherenkov (RICH) [33] detectors used for the
 97 particle identification (PID) [34,35], whose performance of
 98 simulated samples is calibrated to match that evaluated with
 99 high-yield decay modes in data. The Λ_b^0/Ξ_b^0 decays are
 100 selected by an online trigger system which consists of a
 101 hardware stage followed by a software stage [35,36]. The
 102 hardware trigger is based on information from the calorimeter
 103 and muon systems. The software trigger applies full
 104 event reconstruction, selecting events with a two-, three- or
 105 four-track secondary vertex with a significant displacement
 106 from any primary pp interaction vertex. Simulated
 107 $\Lambda_b^0/\Xi_b^0 \rightarrow \Lambda h^+ h'^-$ decays are used to model the effects of
 108 the detector acceptance and imposed selection requirements,
 109 and the signal mass distributions. In the simulation, samples
 110 are generated with PYTHIA [37], EvtGen [38], PHOTOS [39],
 111 and the Geant4 toolkits [40] as described in Ref. [41].

112 In the offline selection, tracks identified as a proton and a
 113 pion are used to form a Λ candidate, which is further
 114 combined with a pair of oppositely charged hadrons

identified as a pion or kaon to form a Λ_b^0/Ξ_b^0 candidate.
 Backgrounds from specific narrow resonances including
 $K_S^0, D^0, \Lambda_c^+, \Xi_c^+, J/\psi$, and χ_{c0} hadrons formed by combinations of tracks from the final state particles of Λ_b^0/Ξ_b^0 candidates are removed by vetoing in the relevant mass spectra. Further discrimination of signal from background is achieved through a boosted decision tree (BDT) classifier [42,43], using a combination of kinematic and topological variables as inputs. The BDT classifier is trained with simulated $\Lambda_b^0 \rightarrow \Lambda \pi^+ \pi^-$ decays as the signal, and using the data sample in the mass region $m(\Delta \pi^+ \pi^-) \in [5800, 6100] \text{ MeV}/c^2$ as the background. Requirements on the BDT response and PID of final-state tracks are optimized and applied simultaneously to maximize the figure-of-merit, defined as $N_S / \sqrt{N_S + N_B}$ [$N_S / (\sqrt{N_B} + 2.5)$] for the Λ_b^0 (Ξ_b^0) decays. Here N_S and N_B are the signal and background yields in the Λ_b^0 (Ξ_b^0) signal region, defined as a $\pm 50 \text{ MeV}/c^2$ mass window around the known Λ_b^0 (Ξ_b^0) mass [44]. The PID requirements help to reduce combinatorial background and cross feeds from other signal decays and from B -meson decays. The contributions from B -meson decays are suppressed to a negligible level.

The $\Lambda h^+ h'^-$ mass distributions after all selections are shown in Fig. 5 of the End Matter, together with fit projections. The obtained signal yields are summarized in Table I, extracted using a simultaneous unbinned maximum-likelihood fit to all the $\Lambda h^+ h'^-$ mass distributions, where the two CP conjugate states are combined. The signal component in the corresponding $\Lambda h^+ h'^-$ mass distribution is modeled by the sum of two Crystal Ball (CB) functions [45], with tail parameters fixed from simulation. The distributions of cross feeds from other signal decays due to misidentified h^+ or h'^- hadrons are obtained from simulation, and their yields are constrained to the respective yields of the correctly reconstructed signals multiplied by the experimental efficiencies evaluated from simulation. The decay $\Lambda_b^0 \rightarrow \Lambda h^+ h'^- \gamma/\pi^0$, with γ/π^0 not reconstructed, is modeled by an ARGUS function [46] convolved by a Gaussian distribution for the experimental resolution. The shape parameters of ARGUS function are constrained from

TABLE I. Signal yield and (upper limit of) CP -averaged branching fraction (\mathcal{B}) for each decay mode. The uncertainties are statistical, systematic, and due to the branching fraction of the control mode. The yield for the control mode is also shown.

Decay	Yield	$\mathcal{B} (\times 10^{-6})$
$\Lambda_b^0 \rightarrow \Lambda \pi^+ \pi^-$	$(6.36 \pm 0.42) \times 10^2$	$5.3 \pm 0.4 \pm 0.5 \pm 0.5$
$\Lambda_b^0 \rightarrow \Lambda K^+ \pi^-$	$(6.18 \pm 0.32) \times 10^2$	$4.6 \pm 0.2 \pm 0.4 \pm 0.5$
$\Lambda_b^0 \rightarrow \Lambda K^+ K^-$	$(1.92 \pm 0.05) \times 10^3$	$10.7 \pm 0.3 \pm 0.4 \pm 1.1$
$\Xi_b^0 \rightarrow \Lambda \pi^+ \pi^-$	$(5.6 \pm 2.7) \times 10^1$	$11.0 \pm 2.6 \pm 1.4 \pm 3.8$
$\Xi_b^0 \rightarrow \Lambda K^- \pi^+$	$(1.19 \pm 0.15) \times 10^2$	$10.4 \pm 1.4 \pm 1.2 \pm 3.5$
$\Xi_b^0 \rightarrow \Lambda K^+ K^-$	$(1.2 \pm 0.9) \times 10^1$	$< 2.4 \text{ (2.8) at 90\% (95\%) CL}$
$\Lambda_b^0 \rightarrow \Lambda_c^+ (\rightarrow \Lambda \pi^+) \pi^-$	$(5.25 \pm 0.07) \times 10^3$...

simulation. The combinatorial background is modeled by an exponential function. For CP -violation measurements, the signal and background shape parameters are shared between baryon and antibaryon decays while their yields are independent.

Using Wilks's theorem [47], the statistical significances of the $\Lambda_b^0 \rightarrow \Lambda\pi^+\pi^-$ and $\Xi_b^0 \rightarrow \Lambda K^-\pi^+$ decays are measured to be more than 10σ , giving the first observation of these decays. The significance of the $\Xi_b^0 \rightarrow \Lambda\pi^+\pi^-$ decay is determined to be 4.0σ , while that of the $\Xi_b^0 \rightarrow \Lambda K^+K^-$ decay is about 1.7σ .

The branching-fraction (\mathcal{B}) ratio of a signal decay to that of the control mode is measured according to

$$\frac{\mathcal{B}(\Lambda_b^0/\Xi_b^0 \rightarrow \Lambda h^+h'^-)}{\mathcal{B}(\Lambda_b^0 \rightarrow \Lambda_c^+(\rightarrow \Lambda\pi^+)\pi^-)} = \frac{N_{\Lambda_b^0/\Xi_b^0 \rightarrow \Lambda h^+h'^-}}{N_{\Lambda_b^0 \rightarrow \Lambda_c^+(\rightarrow \Lambda\pi^+)\pi^-}} \times \frac{\epsilon_{\Lambda_b^0 \rightarrow \Lambda_c^+(\rightarrow \Lambda\pi^+)\pi^-}}{\epsilon_{\Lambda_b^0/\Xi_b^0 \rightarrow \Lambda h^+h'^-}} \times \frac{f_{\Lambda_b^0}}{f_{\Lambda_b^0/\Xi_b^0}}, \quad (1)$$

where N and ϵ are the yield and efficiency for the considered decay, respectively, and the final factor is the ratio of b -quark fragmentation fractions [48,49]. The yields are determined through the fit to data while the efficiencies are determined from simulation. In the simulation the p_T and rapidity distributions of the Λ_b^0 baryon [50], as well as the Dalitz plot of the Λ_b^0/Ξ_b^0 decays, are corrected to match those in data. The efficiencies are at the level of 10^{-4} , with the efficiency ratio in the range 0.8–2.9 depending on the signal channel. For Ξ_b^0 decays, due to the limited data sample, the p_T and rapidity are not corrected and a 10% systematic uncertainty is assigned to the efficiency.

The branching-fraction results are summarized in Table I, where the uncertainties are statistical, systematic, and due to the uncertainty of the control channel branching fraction [48,51]. As no significant contribution from the $\Xi_b^0 \rightarrow \Lambda K^+K^-$ decay is found, upper limits are determined on its branching fraction at 90% and 95% confidence levels (CL), by integrating the positive side of the profile likelihood [52].

Four channels with sufficiently high yields, including three Λ_b^0 decay modes and the $\Xi_b^0 \rightarrow \Lambda K^-\pi^+$ decay mode, are selected for further investigation of CP violation. The CP asymmetry of the decay to a final state f is defined as

$$\mathcal{A}^{CP}(\Lambda_b^0/\Xi_b^0 \rightarrow f) \equiv \frac{\Gamma(\Lambda_b^0/\Xi_b^0 \rightarrow f) - \Gamma(\bar{\Lambda}_b^0/\bar{\Xi}_b^0 \rightarrow \bar{f})}{\Gamma(\Lambda_b^0/\Xi_b^0 \rightarrow f) + \Gamma(\bar{\Lambda}_b^0/\bar{\Xi}_b^0 \rightarrow \bar{f})}, \quad (2)$$

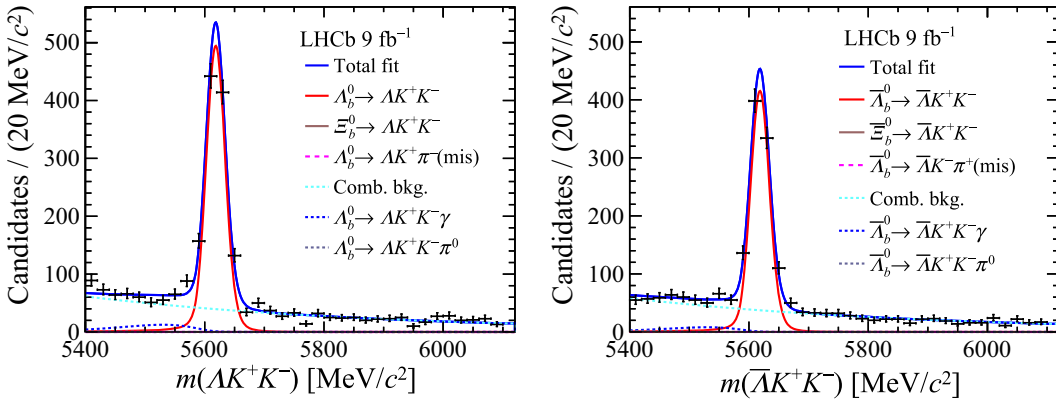
where Γ is the partial decay rate defined without inclusion of its charge-conjugate process. The raw asymmetry of signal yields between baryon and antibaryon decays, denoted as $\mathcal{A}_{\text{raw}}^{CP}$, is first extracted directly from the mass

fits. This is then corrected to account for two factors: the asymmetry of the baryon and antibaryon production rates, A_P , and the asymmetry of the final-state detection and selection efficiencies, A_{exp} [13]. To reduce systematic uncertainties, the difference between the CP asymmetry of each signal decay and the $\Lambda_b^0 \rightarrow \Lambda_c^+(\Lambda\pi^+)\pi^-$ decay, $\Delta\mathcal{A}^{CP} = A_{\text{raw}}(\text{signal}) - A_{\text{raw}}(\text{control}) - \Delta A_P - \Delta A_{\text{exp}}$, is measured, where ΔA_P and ΔA_{exp} represent the production and detection asymmetry difference between signal mode and control mode. Assuming there is no CP violation for the control mode [53], valid within the experimental uncertainties of this analysis, $\Delta\mathcal{A}^{CP}$ gives the measurement of the CP asymmetry for the signal decay.

The Λ_b^0 production asymmetries in pp collisions at $\sqrt{s} = 7$ and 8 TeV have previously been measured at LHCb [54,55], but there is no equivalent measurement yet at $\sqrt{s} = 13$ TeV. As the Λ_b^0 production asymmetry is expected to be smaller at higher energies and mostly cancels between the signal and control channel, the A_P measured for $\sqrt{s} = 8$ TeV is used for the $\Delta\mathcal{A}^{CP}(\Lambda_b^0)$ measurements at $\sqrt{s} = 13$ TeV. Assuming isospin symmetry between the Ξ_b^0 and Ξ_b^- cross-sections in pp collisions, the Ξ_b^0 production asymmetry is taken to be the same as that of the Ξ_b^- baryon, which has been measured by the LHCb experiment [49]. The detection asymmetry encompasses the asymmetries in the final-state reconstruction, the trigger selection and the PID selection. The reconstruction asymmetries for pions, kaons and protons have been measured as a function of particle momenta using control samples of $D^+ \rightarrow K_S^0\pi^+$, $D^+ \rightarrow K^-\pi^+\pi^+$, $D^{*+} \rightarrow D^0(\rightarrow K^-\pi^+\pi^+\pi^-)\pi^+$ decays [56], and simulated samples of $\Lambda_b^0 \rightarrow \Lambda_c^+(\rightarrow pK^-\pi^+)\mu^-\bar{\nu}_\mu$ decays [13]. The detection asymmetry for each final-state particle is then weighted by its momentum distribution in the signal and control modes to get an averaged result, accounting for the kinematics of both modes. The PID and trigger selection asymmetries are obtained in a similar way using data [34,35]. The largest detection asymmetry, due to proton reconstruction, mostly cancels between the signal and control modes. These correction terms ΔA_P and ΔA_{exp} are shown in Table IV in the End Matter, and are all consistent with zero for Λ_b^0 decays with uncertainties around 0.002 and 0.010, respectively. The $\Delta\mathcal{A}^{CP}$ quantities, integrated over the phase space, are measured for the four decays to be

$$\begin{aligned} \Delta\mathcal{A}^{CP}(\Lambda_b^0 \rightarrow \Lambda\pi^+\pi^-) &= -0.013 \pm 0.053 \pm 0.018, \\ \Delta\mathcal{A}^{CP}(\Lambda_b^0 \rightarrow \Lambda K^+\pi^-) &= -0.118 \pm 0.045 \pm 0.021, \\ \Delta\mathcal{A}^{CP}(\Lambda_b^0 \rightarrow \Lambda K^+K^-) &= 0.083 \pm 0.023 \pm 0.016, \\ \Delta\mathcal{A}^{CP}(\Xi_b^0 \rightarrow \Lambda K^-\pi^+) &= 0.27 \pm 0.12 \pm 0.05, \end{aligned}$$

where the first uncertainties are statistical and the second are systematic. The $\Delta\mathcal{A}^{CP}$ measurement for the $\Lambda_b^0 \rightarrow \Lambda K^+K^-$ decay has a significance of 3.1σ based on the negative log-



F1:1

FIG. 1. Mass distributions of (left) $\Lambda_b^0 \rightarrow \Lambda K^+ K^-$ and (right) $\bar{\Lambda}_b^0 \rightarrow \bar{\Lambda} K^+ K^-$ decays, with the fit projections.

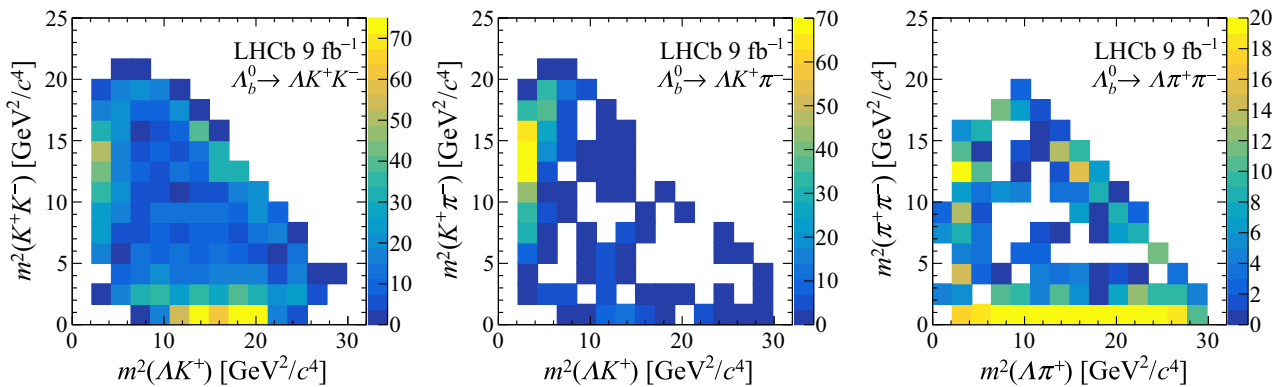
likelihood method [57], accounting for both statistical and systematic uncertainties. This significance is confirmed by using ensembles of pseudoexperiments.

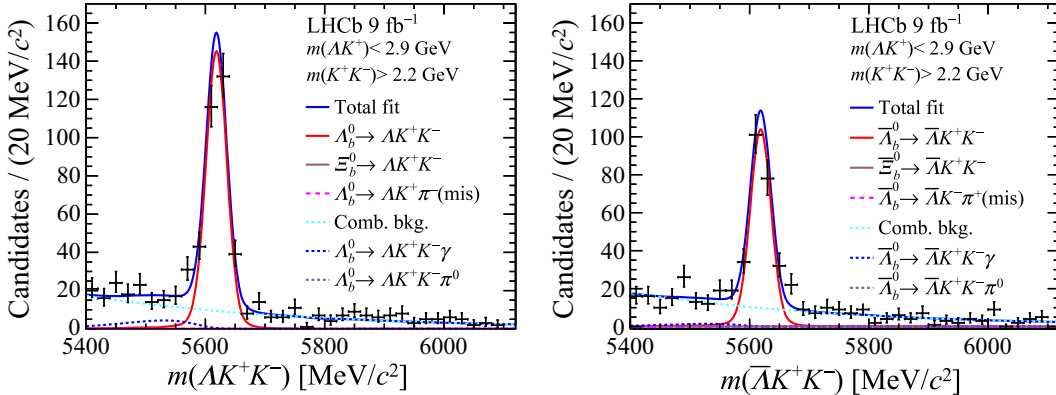
The mass distributions of $\Lambda_b^0 \rightarrow \Lambda K^+ K^-$ for both baryon and antibaryon decays, with fit results also plotted, are shown in Fig. 1 where a clear difference in signal yields between Λ_b^0 and $\bar{\Lambda}_b^0$ decays can be seen. The decay is dominated by intermediate $N^{*+}(\rightarrow \Lambda K^+)$ or $\phi(\rightarrow K^+ K^-)$ resonances, as can be seen in the $\Lambda_b^0 \rightarrow \Lambda K^+ K^-$ Dalitz plot of Fig. 2 (left), where background contributions are subtracted using the *sPlot* technique [58]. To investigate whether these resonances are the source of the CP asymmetry, separate $\Delta\mathcal{A}^{CP}$ measurements are performed within these two resonance-dominated regions. In the region dominated by the N^{*+} resonance, the asymmetry is determined to be $\Delta\mathcal{A}^{CP} = 0.165 \pm 0.048 \pm 0.017$, which differs from zero by 3.2σ . The mass distributions of the $\Lambda_b^0 \rightarrow \Lambda K^+ K^-$ and $\bar{\Lambda}_b^0 \rightarrow \bar{\Lambda} K^+ K^-$ decays and their fit projections, within the region, are shown in Fig. 3, demonstrating the difference between Λ_b^0 and $\bar{\Lambda}_b^0$ yields. The CP asymmetry in the ϕ region is consistent with zero. A potential variation of the CP asymmetry across the Dalitz

plot is also studied in 10 equally populated Dalitz bins using an adaptive binning scheme [19,59]. The results are consistent with CP symmetry.

The significances for CP violation in $\Lambda_b^0 \rightarrow \Lambda K^+ \pi^-$, $\Lambda_b^0 \rightarrow \Lambda \pi^+ \pi^-$ and $\Xi_b^0 \rightarrow \Lambda K^- \pi^+$ decays are 2.4σ , 0.2σ and 2.1σ , respectively. The detailed mass distributions for both their baryon and antibaryon decays can be found in supplementary material [61]. Further searches for CP violation are also performed for the two Λ_b^0 decays both in resonance-dominated regions [see Fig. 2 (middle, right) and Table II] and with an adaptive binning scheme. The results are all consistent with CP symmetry. For the Ξ_b^0 decays, no localized CP asymmetry searches are performed due to the low signal yields.

Cross-checks are performed to investigate the stability of the branching fraction and $\Delta\mathcal{A}^{CP}$ measurements. For the global asymmetries and branching fractions, results are obtained in different data-taking periods, as well as with different magnet polarities, and are found to be consistent. For the measurements in different resonance-dominated regions, alternative definitions of the mass regions are used, and similar results as the nominal ones are obtained.

F2:1
F2:2
F2:3FIG. 2. Dalitz plots of (left) $\Lambda_b^0 \rightarrow \Lambda K^+ K^-$, (middle) $\Lambda_b^0 \rightarrow \Lambda K^+ \pi^-$, (right) $\Lambda_b^0 \rightarrow \Lambda \pi^+ \pi^-$ decays. Background contributions are subtracted using the *sPlot* technique. The coordinates are calculated after a kinematic fit which constrains the Λ_b^0 and Λ baryon masses to their known values [44].



F3:1 FIG. 3. Mass distributions of (left) $\Lambda_b^0 \rightarrow \Lambda K^+ K^-$ and (right) $\bar{\Lambda}_b^0 \rightarrow \bar{\Lambda} K^+ K^-$ decays in N^* resonance-dominated regions. Also shown
F3:2 are the fit results.

289 Various sources of systematic uncertainties on the
290 branching fraction and $\Delta\mathcal{A}^{CP}$ measurements are considered.
291 The uncertainty due to the imperfect modelling of
292 the mass distributions is evaluated by using alternative
293 models for each component, including an Hypatia function
294 [60] for the signal model and a second-order polynomial
295 function for the combinatorial background. For the
296 $\Delta\mathcal{A}^{CP}$ measurements, an additional uncertainty arises
297 from using shared fit parameters for baryon and anti-
298 baryon decays. This is assessed by removing this con-
299 straint and assigning the resulting $\Delta\mathcal{A}^{CP}$ shifts as
300 systematic uncertainties. The systematic uncertainty from
301 the efficiency ratio has several contributions. The first
302 contribution arises from the finite size of simulation
303 samples, which is propagated to the branching fraction
304 and $\Delta\mathcal{A}^{CP}$ measurements using pseudoexperiments.
305 Another contribution is due to the robustness of efficiency
306 corrections, which are studied in alternative scenarios. For
307 example, the effect of the vetoing of charm hadrons is
308 studied by varying the vetoed mass regions, a new
309 efficiency map is obtained to calculate the corresponding
310 branching fraction and the difference is taken as a
311 systematic uncertainty. The uncertainties on the produc-
312 tion and experimental asymmetries are propagated to the
313 $\Delta\mathcal{A}^{CP}$ measurements using pseudoexperiments and
314 largely cancel in the difference of signal and control
315 mode asymmetries. The total systematic uncertainties are
316 obtained by summing all contributions in quadrature.

In summary, $\Lambda_b^0/\Xi_b^0 \rightarrow \Lambda h^+ h'^-$ decays are studied using pp collision data collected by the LHCb experiment during LHC Runs 1–2. The $\Lambda_b^0 \rightarrow \Lambda\pi^+\pi^-$ and $\Xi_b^0 \rightarrow \Lambda K^-\pi^+$ decays are observed for the first time, and evidence is also found for the $\Xi_b^0 \rightarrow \Lambda\pi^+\pi^-$ decay. The branching-fraction measurements of $\Lambda_b^0/\Xi_b^0 \rightarrow \Lambda h^+ h'^-$ decays are more precise than and supersede previous LHCb results [11]. The CP asymmetries are measured for $\Lambda_b^0 \rightarrow \Lambda h^+ h'^-$ and $\Xi_b^0 \rightarrow \Lambda K^-\pi^+$ decays, with respect to the $\Lambda_b^0 \rightarrow \Lambda_c^+(\rightarrow \Lambda\pi^+)\pi^-$ decay. Evidence for CP violation is found in the $\Lambda_b^0 \rightarrow \Lambda K^+ K^-$ decay for the first time, with $\Delta\mathcal{A}^{CP} = (8.3 \pm 2.8)\%$ integrated over the final-state phase space. The CP asymmetry is enhanced in the N^{*+} mass region, where it is measured to be $\Delta\mathcal{A}^{CP} = (16.5 \pm 5.1)\%$. No evidence of CP violation is found for other Λ_b^0/Ξ_b^0 decays studied. These measurements represent an important step towards establishing CP violation in baryon decays, setting the stage for future studies of quasi-two-body decays.

Acknowledgments—We express our gratitude to our colleagues in the CERN accelerator departments for the excellent performance of the LHC. We thank the technical and administrative staff at the LHCb institutes. We acknowledge support from CERN and from the national agencies: CAPES, CNPq, FAPERJ, and FINEP (Brazil); MOST and NSFC (China); CNRS/IN2P3 (France); BMBF, DFG, and MPG (Germany); INFN (Italy); NWO (Netherlands); MNiSW and NCN (Poland); MCID/IFA

TABLE II. Definitions of the resonance-dominated regions and the corresponding $\Delta\mathcal{A}^{CP}$ values. The symbol f represents multiple resonances at low $\pi^+\pi^-$ mass.

Channel	$m(h^+h'^-)$	$m(\Lambda h^+)$	$\Delta\mathcal{A}^{CP}$
$\Lambda_b^0 \rightarrow \Lambda\phi(\rightarrow K^+K^-)$	$< 1.10 \text{ GeV}/c^2$...	$0.150 \pm 0.055 \pm 0.021$
$\Lambda_b^0 \rightarrow N^{*+}(\rightarrow \Lambda K^+)K^-$	$> 2.20 \text{ GeV}/c^2$	$< 2.90 \text{ GeV}/c^2$	$0.165 \pm 0.048 \pm 0.017$
$\Lambda_b^0 \rightarrow N^{*+}(\rightarrow \Lambda K^+)\pi^-$...	$< 2.30 \text{ GeV}/c^2$	$-0.078 \pm 0.051 \pm 0.027$
$\Lambda_b^0 \rightarrow \Lambda f(\rightarrow \pi^+\pi^-)$	$< 1.70 \text{ GeV}/c^2$...	$0.088 \pm 0.069 \pm 0.021$

(Romania); MICIU and AEI (Spain); SNSF and SER (Switzerland); NASU (Ukraine); STFC (United Kingdom); DOE NP and NSF (USA). We acknowledge the computing resources that are provided by CERN, IN2P3 (France), KIT and DESY (Germany), INFN (Italy), SURF (Netherlands), PIC (Spain), GridPP (United Kingdom), CSCS (Switzerland), IFIN-HH (Romania), CBPF (Brazil), and Polish WLCG (Poland). We are indebted to the communities behind the multiple open-source software packages on which we depend. Individual groups or members have received support from ARC and ARDC (Australia); Key Research Program of Frontier Sciences of CAS, CAS PIFI, CAS CCEPP, Fundamental Research Funds for the Central Universities, and Sci. & Tech. Program of Guangzhou (China); Minciencias (Colombia); EPLANET, Marie Skłodowska-Curie Actions, ERC and NextGenerationEU (European Union); A*MIDEX, ANR, IPhU and Labex P2IO, and Région Auvergne-Rhône-Alpes (France); AvH Foundation (Germany); ICSC (Italy); Severo Ochoa and María de Maeztu Units of Excellence, GVA, XuntaGal, GENCAT, InTalent-Inditex and Prog. Atracción Talento CM (Spain); SRC (Sweden); the Leverhulme Trust, the Royal Society and UKRI (United Kingdom).

- [16] R. Aaij *et al.* (LHCb Collaboration), *Phys. Lett. B* **759**, 282 (2016).
- [17] R. Aaij *et al.* (LHCb Collaboration), *J. High Energy Phys.* **03** (2018) 182.
- [18] R. Aaij *et al.* (LHCb Collaboration), *Eur. Phys. J. C* **80**, 986 (2020).
- [19] R. Aaij *et al.* (LHCb Collaboration), *Phys. Rev. D* **108**, 012008 (2023).
- [20] R. Aaij *et al.* (LHCb Collaboration), *Phys. Rev. Lett.* **123**, 231802 (2019).
- [21] R. Aaij *et al.* (LHCb Collaboration), *Phys. Rev. D* **90**, 112004 (2014).
- [22] C. Q. Geng, Y. K. Hsiao, Y.-H. Lin, and Y. Yu, *Eur. Phys. J. C* **76**, 399 (2016).
- [23] S. Arunagiri and C. Q. Geng, *Phys. Rev. D* **69**, 017901 (2004).
- [24] X.-H. Guo and A. W. Thomas, *Phys. Rev. D* **58**, 096013 (1998).
- [25] J. Zhu, Z.-T. Wei, and H.-W. Ke, *Phys. Rev. D* **99**, 054020 (2019).
- [26] Z. Rui, J.-M. Li, and C.-Q. Zhang, *Phys. Rev. D* **107**, 053009 (2023).
- [27] Y. K. Hsiao, Y. Yao, and C. Q. Geng, *Phys. Rev. D* **95**, 093001 (2017).
- [28] J.-P. Wang and F.-S. Yu, *Chin. Phys. C* **48**, 101001 (2024).
- [29] A. A. Alves Jr. *et al.* (LHCb Collaboration), *J. Instrum.* **3**, S08005 (2008).
- [30] R. Aaij *et al.* (LHCb Collaboration), *Int. J. Mod. Phys. A* **30**, 1530022 (2015).
- [31] R. Arink *et al.*, *J. Instrum.* **9**, P01002 (2014).
- [32] P. d'Argent *et al.*, *J. Instrum.* **12**, P11016 (2017).
- [33] M. Adinolfi *et al.*, *Eur. Phys. J. C* **73**, 2431 (2013).
- [34] L. Anderlini, A. Contu, C. R. Jones, S. S. Malde, D. Muller, S. Ogilvy, J. M. Otalora Goicochea, A. Pearce, I. Polyakov, W. Qian, B. Sciascia, R. Vazquez Gomez, and Y. Zhang, The PIDCalib package (2016), <http://cds.cern.ch/record/2202412>.
- [35] R. Aaij *et al.*, *J. Instrum.* **14**, P04013 (2019).
- [36] R. Aaij *et al.*, *J. Instrum.* **8**, P04022 (2013).
- [37] T. Sjöstrand, S. Mrenna, and P. Skands, *Comput. Phys. Commun.* **178**, 852 (2008); *J. High Energy Phys.* **05** (2006) 026.
- [38] D. J. Lange, *Nucl. Instrum. Methods Phys. Res., Sect. A* **462**, 152 (2001).
- [39] P. Golonka and Z. Was, *Eur. Phys. J. C* **45**, 97 (2006).
- [40] J. Allison, K. Amako, J. Apostolakis, H. Araujo, P. Dubois *et al.* (Geant4 Collaboration), *IEEE Trans. Nucl. Sci.* **53**, 270 (2006); S. Agostinelli *et al.* (Geant4 Collaboration), *Nucl. Instrum. Methods Phys. Res., Sect. A* **506**, 250 (2003).
- [41] M. Clemencic, G. Corti, S. Easo, C. R. Jones, S. Miglioranzi, M. Pappagallo, and P. Robbe, *J. Phys. Conf. Ser.* **331**, 032023 (2011).
- [42] L. Breiman, J. H. Friedman, R. A. Olshen, and C. J. Stone, *Classification and Regression Trees* (Wadsworth international group, Belmont, California, USA, 1984).
- [43] H. Voss, A. Hoecker, J. Stelzer, and F. Tegenfeldt, *Proc. Sci. ACAT2007* (2007) 040.
- [44] S. Navas *et al.* (Particle Data Group), *Phys. Rev. D* **110**, 030001 (2024).

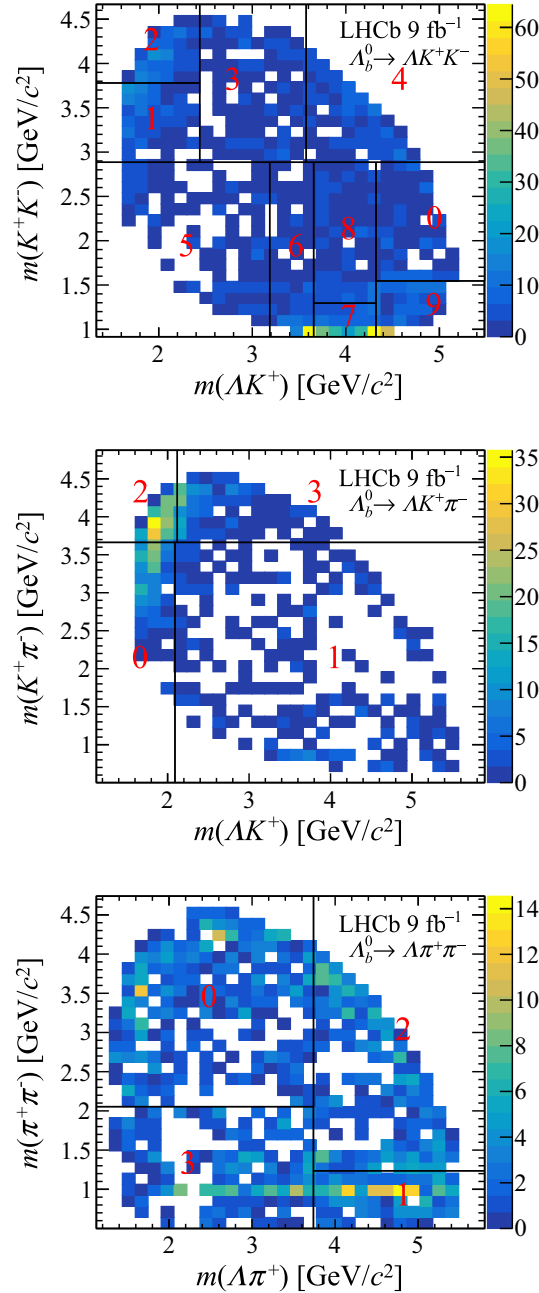
- 462 [45] T. Skwarnicki, A study of the radiative cascade transitions
463 between the Upsilon-prime and Upsilon resonances, Ph.D.
464 thesis, Institute of Nuclear Physics, Krakow, 1986 [Report
465 No. DESY-F31-86-02], <http://inspirehep.net/record/230779/>.
466 [46] H. Albrecht *et al.* (ARGUS Collaboration), *Phys. Lett. B*
467 **241**, 278 (1990).
468 [47] S. S. Wilks, *Ann. Math. Stat.* **9**, 60 (1938).
469 [48] R. Aaij *et al.* (LHCb Collaboration), *J. High Energy Phys.*
470 **08** (2014) 143.
471 [49] R. Aaij *et al.* (LHCb Collaboration), *Phys. Rev. D* **99**,
472 052006 (2019).
473 [50] R. Aaij *et al.* (LHCb Collaboration), *J. High Energy Phys.*
474 **10** (2015) 172.
475 [51] M. Ablikim *et al.* (BESIII Collaboration), *Phys. Rev. Lett.*
476 **116**, 052001 (2016).
477 [52] R. Aaij *et al.* (LHCb Collaboration), *Phys. Rev. D* **108**,
478 012007 (2023).
479 [53] R. Aaij *et al.* (LHCb Collaboration), *Phys. Rev. Lett.* **133**,
480 261804 (2024).
481 [54] R. Aaij *et al.* (LHCb Collaboration), *Phys. Lett. B* **774**, 139
482 (2017).
483 [55] R. Aaij *et al.* (LHCb Collaboration), *J. High Energy Phys.*
484 **10** (2021) 060.
485 [56] R. Aaij *et al.* (LHCb Collaboration), *J. High Energy Phys.*
486 **07** (2014) 041.
487 [57] R. Aaij *et al.* (LHCb Collaboration), *Phys. Rev. D* **110**,
488 032001 (2024).
489 [58] M. Pivk and F. R. Le Diberder, *Nucl. Instrum. Methods*
490 *Phys. Res., Sect. A* **555**, 356 (2005).
491 [59] I. Bediaga, J. Miranda, A. C. dos Reis, I. I. Bigi, A. Gomes,
492 J. M. Otalora Goicochea, and A. Veiga, *Phys. Rev. D* **86**,
493 036005 (2012).
494 [60] D. Martínez Santos and F. Dupertuis, *Nucl. Instrum.*
495 *Methods Phys. Res., Sect. A* **764**, 150 (2014).
496 [61] See Supplemental Material at [http://link.aps.org/
497 supplemental/10.1103/PhysRevLett.000.000000](http://link.aps.org/supplemental/10.1103/PhysRevLett.000.000000) more details
498 for the fit results of the ACP measurements. **Q1** 498

End Matter

501 *Appendix A: Summary figures and tables for the*
502 *adaptive binning scheme*—Figure 4 shows the two-
503 dimensional mass distributions for (top) $\Lambda_b^0 \rightarrow \Lambda K^+ K^-$,
504 (middle) $\Lambda_b^0 \rightarrow \Lambda K^+ \pi^-$, and (bottom) $\Lambda_b^0 \rightarrow \Lambda \pi^+ \pi^-$,
505 along with the bin boundaries used for the adaptive
506 binning scheme. Table III lists the bin definitions used
507 for each decay mode and the per-bin *CP* asymmetry
508 measurements.

509 *Appendix B: Summary for correction terms*—Table IV
510 lists the production asymmetry difference ΔA_P and
511 detection asymmetry difference ΔA_{exp} for each decay
512 mode with respect to control mode. The central value of
513 Λ_b^0 absolute A_P is at the level of 1% [55].
527
528

514 *Appendix C: Summary of the fit results*—Figure 5
515 shows the mass spectra used to obtain yields of signal
516 channels for BF calculations of (top) $\Lambda_b^0(\Xi_b^0) \rightarrow \Lambda K^+ K^-$,
517 (middle left) $\Lambda_b^0 \rightarrow \Lambda K^+ \pi^-$, (middle right)
518 $\Xi_b^0 \rightarrow \Lambda K^- \pi^+$, and (bottom) $\Lambda_b^0(\Xi_b^0) \rightarrow \Lambda K^+ K^-$ decay
519 modes. The same BDT classifier is used in selections
520 for the Λ_b^0 and Ξ_b^0 modes, but with a different figure-of-
521 merit (FoM). Because of the relatively smaller number
522 of Ξ_b^0 signal yields, when determining its selection
523 criteria the $N_S/(\sqrt{N_B} + 2.5)$ FoM method is applied, as
524 shown in Fig. 5 (right), whereas when studying the Λ_b^0
525 modes, the $N_S/\sqrt{N_S + N_B}$ FoM method is applied, as
526 shown in Fig. 5 (left).



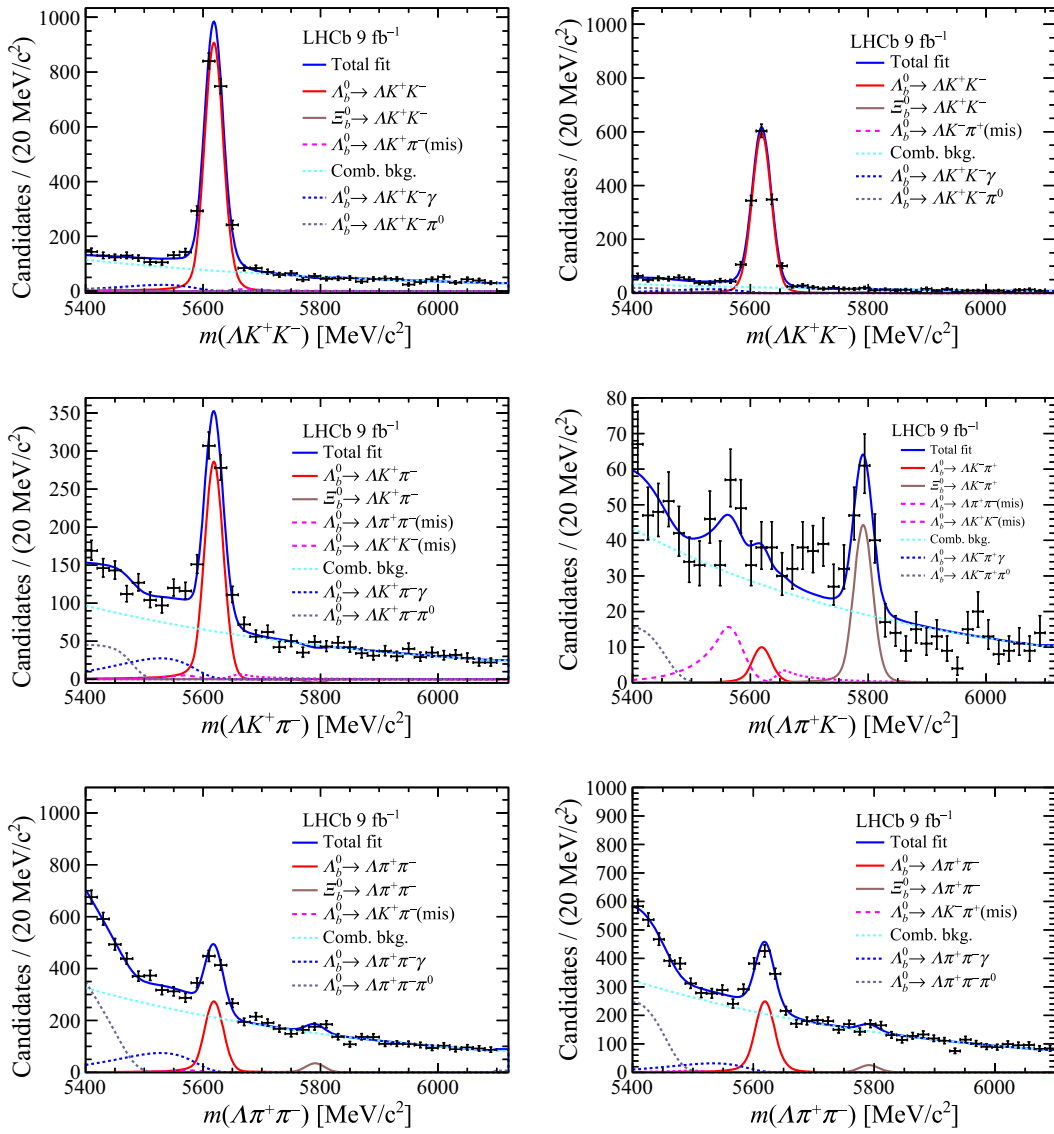
F4:1 FIG. 4. Two-dimensional mass distributions for (top) $\Lambda_b^0 \rightarrow \Lambda K^+ K^-$, (middle) $\Lambda_b^0 \rightarrow \Lambda K^+ \pi^-$, and (bottom) $\Lambda_b^0 \rightarrow \Lambda\pi^+\pi^-$ decays in
F4:2 data. The boundaries for the adaptive binning scheme are drawn as solid lines.

TABLE III. Boundaries of the adaptive binning scheme and the $\Delta\mathcal{A}^{CP}$ measurements from each bin, the first uncertainty is statistical and the second is systematic. The variables of the x and y axes and the bin numbers in the table are those presented in Fig. 4. The reported ranges are expressed in GeV/c^2 .

Channel	Bin number	x low	x high	y low	y high	$\Delta\mathcal{A}^{CP}$
$\Lambda_b^0 \rightarrow \Lambda\pi^+\pi^-$	0	1.13	3.74	2.05	4.74	$-0.483 \pm 0.200 \pm 0.043$
	1	3.74	5.50	0.50	1.24	$0.147 \pm 0.092 \pm 0.026$
	2	3.74	5.50	1.24	4.74	$0.058 \pm 0.114 \pm 0.028$
	3	1.13	3.74	0.50	2.05	$0.067 \pm 0.111 \pm 0.028$
	0	1.13	2.09	0.50	3.66	$-0.153 \pm 0.079 \pm 0.027$
	1	2.09	5.49	0.50	3.66	$-0.284 \pm 0.188 \pm 0.041$
	2	1.13	2.12	3.66	4.87	$-0.006 \pm 0.062 \pm 0.028$
	3	2.12	5.49	3.66	4.87	$-0.264 \pm 0.125 \pm 0.030$
	0	4.32	5.08	1.55	2.88	$0.017 \pm 0.092 \pm 0.025$
	1	1.33	2.44	2.88	3.78	$0.188 \pm 0.075 \pm 0.023$
$\Lambda_b^0 \rightarrow \Lambda K^+ \pi^-$	2	1.33	2.44	3.78	4.67	$0.062 \pm 0.077 \pm 0.022$
	3	2.44	3.58	2.88	4.67	$0.064 \pm 0.093 \pm 0.024$
	4	3.58	5.08	2.88	4.67	$0.088 \pm 0.077 \pm 0.022$
	5	1.33	3.19	0.92	2.88	$0.061 \pm 0.089 \pm 0.024$
	6	3.19	3.66	0.92	2.88	$0.066 \pm 0.088 \pm 0.024$
	7	3.66	4.32	0.92	1.30	$0.168 \pm 0.070 \pm 0.021$
	8	3.66	4.32	1.30	2.88	$-0.002 \pm 0.080 \pm 0.023$
	9	4.32	5.08	0.92	1.55	$0.025 \pm 0.074 \pm 0.022$

TABLE IV. Production asymmetry difference ΔA_P and detection asymmetry difference ΔA_{exp} for each decay mode. The uncertainties from these asymmetries are propagated into the phase-space integrated $\Delta\mathcal{A}^{CP}$ as systematic uncertainties.

Channel	ΔA_P (%)	ΔA_{exp} (%)
$\Lambda_b^0 \rightarrow \Lambda\pi^+\pi^-$	0.1 ± 0.1	0.1 ± 0.9
$\Lambda_b^0 \rightarrow \Lambda K^+ \pi^-$	0.2 ± 0.2	1.4 ± 1.0
$\Lambda_b^0 \rightarrow \Lambda K^+ K^-$	-0.2 ± 0.2	0.0 ± 0.9
$\Xi_b^0 \rightarrow \Lambda K^- \pi^+$	-5.2 ± 4.0	0.3 ± 1.6



F5:1 FIG. 5. Distributions of $m(\Lambda h^+h^-)$ for (top left)(top right) $\Lambda_b^0(\Xi_b^0) \rightarrow \Lambda K^+ K^-$, (middle left) $\Lambda_b^0 \rightarrow \Lambda K^+ \pi^-$, (middle right)
F5:2 $\Xi_b^0 \rightarrow \Lambda K^- \pi^+$, and (bottom left)(bottom right) $\Lambda_b^0(\Xi_b^0) \rightarrow \Lambda K^+ K^-$ decay modes, together with the fit results, where (top left)(middle
F5:3 left)(bottom left) are selected with the $N_S / (\sqrt{N_B + N_S})$ FoM, focusing on the Λ_b^0 studies, while (top right)(middle right)(bottom right)
F5:4 are selected with the $N_S / (\sqrt{N_B} + 2.5)$ FoM. for Ξ_b^0 studies.

530

531 R. Aaij³⁸, A. S. W. Abdelmotteleb⁵⁷, C. Abellan Beteta⁵¹, F. Abudinén⁵⁷, T. Ackernley⁶¹, A. A. Adefisoye⁶⁹,
532 B. Adeva⁴⁷, M. Adinolfi⁵⁵, P. Adlarson⁸², C. Agapoulou¹⁴, C. A. Aidala⁸³, Z. Ajaltouni,¹¹ S. Akar⁶⁶,
533 K. Akiba³⁸, P. Albicocco²⁸, J. Albrecht^{19,b}, F. Alessio⁴⁹, M. Alexander⁶⁰, Z. Aliouche⁶³, P. Alvarez Cartelle⁵⁶,
534 R. Amalric¹⁶, S. Amato³, J. L. Amey⁵⁵, Y. Amhis¹⁴, L. An⁶, L. Anderlini²⁷, M. Andersson⁵¹,
535 A. Andreianov⁴⁴, P. Andreola⁵¹, M. Andreotti²⁶, D. Andreou⁶⁹, A. Anelli^{31,c}, D. Ao⁷, F. Archilli^{37,d},
536 M. Argenton²⁶, S. Arguedas Cuendis^{9,49}, A. Artamonov⁴⁴, M. Artuso⁶⁹, E. Aslanides¹³, R. Ataíde Da Silva⁵⁰,
537 M. Atzeni⁶⁵, B. Audurier¹², D. Bacher⁶⁴, I. Bachiller Perea¹⁰, S. Bachmann²², M. Bachmayer⁵⁰, J. J. Back⁵⁷,
538 P. Baladron Rodriguez⁴⁷, V. Balagura¹⁵, A. Balboni²⁶, W. Baldini²⁶, L. Balzani¹⁹, H. Bao⁷,
539 J. Baptista de Souza Leite⁶¹, C. Barbero Pretel^{47,12}, M. Barbetti²⁷, I. R. Barbosa⁷⁰, R. J. Barlow⁶³,
540 M. Barnyakov²⁵, S. Barsuk¹⁴, W. Barter⁵⁹, M. Bartolini⁵⁶, J. Bartz⁶⁹, J. M. Basels¹⁷, S. Bashir⁴⁰, G. Bassi^{35,e}

- B. Batsukh⁵, P. B. Battista¹⁴, A. Bay⁵⁰, A. Beck⁵⁷, M. Becker¹⁹, F. Bedeschi³⁵, I. B. Bediaga²,
 N. A. Behling¹⁹, S. Belin⁴⁷, K. Belous⁴⁴, I. Belov²⁹, I. Belyaev³⁶, G. Benane¹³, G. Bencivenni²⁸,
 E. Ben-Haim¹⁶, A. Berezhnay⁴⁴, R. Bernet⁵¹, S. Bernet Andres⁴⁵, A. Bertolin³³, C. Betancourt⁵¹, F. Betti⁵⁹,
 J. Bex⁵⁶, Ia. Bezshyiko⁵¹, J. Bhom⁴¹, M. S. Bieker¹⁹, N. V. Biesuz²⁶, P. Billoir¹⁶, A. Biolchini³⁸, M. Birch⁶²,
 F. C. R. Bishop¹⁰, A. Bitadze⁶³, A. Bizzeti¹⁰, T. Blake⁵⁷, F. Blanc⁵⁰, J. E. Blank¹⁹, S. Blusk⁶⁹, V. Bocharkov⁴⁴,
 J. A. Boelhauve¹⁹, O. Boente Garcia¹⁵, T. Boettcher⁶⁶, A. Bohare⁵⁹, A. Boldyrev⁴⁴, C. S. Bolognani⁷⁹,
 R. Bolzonella^{26,f}, R. B. Bonacci¹, N. Bondar⁴⁴, A. Bordelius⁴⁹, F. Borgato^{33,g}, S. Borghi⁶³, M. Borsato^{31,c},
 J. T. Borsuk⁴¹, S. A. Bouchiba⁵⁰, M. Bovill⁶⁴, T. J. V. Bowcock⁶¹, A. Boyer⁴⁹, C. Bozzi²⁶, A. Brea Rodriguez⁵⁰,
 N. Breer¹⁹, J. Brodzicka⁴¹, A. Brossa Gonzalo^{47,a}, J. Brown⁶¹, D. Brundu³², E. Buchanan⁵⁹, A. Buonauro⁵¹,
 L. Buonincontri^{33,g}, A. T. Burke⁶³, C. Burr⁴⁹, J. S. Butter⁵⁶, J. Buytaert⁴⁹, W. Byczynski⁴⁹, S. Cadeddu³²,
 H. Cai⁷⁴, A. C. Caillet¹⁶, R. Calabrese^{26,f}, S. Calderon Ramirez⁹, L. Calefice⁴⁶, S. Cali²⁸, M. Calvi^{31,c},
 M. Calvo Gomez⁴⁵, P. Camargo Magalhaes^{2,h}, J. I. Cambon Bouzas⁴⁷, P. Campana²⁸, D. H. Campora Perez⁷⁹,
 A. F. Campoverde Quezada⁷, S. Capelli³¹, L. Capriotti²⁶, R. Caravaca-Mora⁹, A. Carbone^{25,i},
 L. Carcedo Salgado⁴⁷, R. Cardinale^{29,j}, A. Cardini³², P. Carniti^{31,c}, L. Carus²², A. Casais Vidal⁶⁵, R. Caspary²²,
 G. Casse⁶¹, M. Cattaneo⁴⁹, G. Cavallero^{26,49}, V. Cavallini^{26,f}, S. Celani²², D. Cervenkov⁶⁴, S. Cesare^{30,k},
 A. J. Chadwick⁶¹, I. Chahrour⁸³, M. Charles¹⁶, Ph. Charpentier⁴⁹, E. Chatzianagnostou³⁸, M. Chefdeville¹⁰,
 C. Chen¹³, S. Chen⁵, Z. Chen⁷, A. Chernov⁴¹, S. Chernyshenko⁵³, X. Chiotopoulos⁷⁹, V. Chobanova⁸¹,
 S. Cholak⁵⁰, M. Chrzaszcz⁴¹, A. Chubykin⁴⁴, V. Chulikov²⁸, P. Ciambrone²⁸, X. Cid Vidal⁴⁷, G. Ciezarek⁴⁹,
 P. Cifra⁴⁹, P. E. L. Clarke⁵⁹, M. Clemencic⁴⁹, H. V. Cliff⁵⁶, J. Closier⁴⁹, C. Cocha Toapaxi²², V. Coco⁴⁹,
 J. Cogan¹³, E. Cogneras¹¹, L. Cojocariu⁴³, S. Collaviti⁵⁰, P. Collins⁴⁹, T. Colombo⁴⁹, M. Colonna¹⁹,
 A. Comerma-Montells⁴⁶, L. Congedo²⁴, A. Contu³², N. Cooke⁶⁰, I. Corredoira⁴⁷, A. Correia¹⁶, G. Corti⁴⁹,
 J. J. Cottee Meldrum⁵⁵, B. Couturier⁴⁹, D. C. Craik⁵¹, M. Cruz Torres^{2,1}, E. Curras Rivera⁵⁰, R. Currie⁵⁹,
 C. L. Da Silva⁶⁸, S. Dadabaev⁴⁴, L. Dai⁷¹, X. Dai⁶, E. Dall'Occo⁴⁹, J. Dalseno⁴⁷, C. D'Ambrosio⁴⁹,
 J. Daniel¹¹, A. Danilina⁴⁴, P. d'Argent²⁴, G. Darze³, A. Davidson⁵⁷, J. E. Davies⁶³, A. Davis⁶³,
 O. De Aguiar Francisco⁶³, C. De Angelis^{32,m}, F. De Benedetti⁴⁹, J. de Boer³⁸, K. De Bruyn⁷⁸, S. De Capua⁶³,
 M. De Cian²², U. De Freitas Carneiro Da Graca^{2,n}, E. De Lucia²⁸, J. M. De Miranda², L. De Paula³,
 M. De Serio^{24,o}, P. De Simone²⁸, F. De Vellis¹⁹, J. A. de Vries⁷⁹, F. Debernardis²⁴, D. Decamp¹⁰, V. Dedu¹³,
 S. Dekkers¹, L. Del Buono¹⁶, B. Delaney⁶⁵, H.-P. Dembinski¹⁹, J. Deng⁸, V. Denysenko⁵¹, O. Deschamps¹¹,
 F. Dettori^{32,m}, B. Dey⁷⁷, P. Di Nezza²⁸, I. Diachkov⁴⁴, S. Didenko⁴⁴, S. Ding⁶⁹, L. Dittmann²², V. Dobishuk⁵³,
 A. D. Docheva⁶⁰, C. Dong^{4,p}, A. M. Donohoe²³, F. Dordei³², A. C. dos Reis², A. D. Dowling⁶⁹, W. Duan⁷²,
 P. Duda⁸⁰, M. W. Dudek⁴¹, L. Dufour⁴⁹, V. Duk³⁴, P. Durante⁴⁹, M. M. Duras⁸⁰, J. M. Durham⁶⁸,
 O. D. Durmus⁷⁷, A. Dziurda⁴¹, A. Dzyuba⁴⁴, S. Easo⁵⁸, E. Eckstein¹⁸, U. Egede¹, A. Egorychev⁴⁴,
 V. Egorychev⁴⁴, S. Eisenhardt⁵⁹, E. Ejopu⁶³, L. Eklund⁸², M. Elashri⁶⁶, J. Ellbracht¹⁹, S. Ely⁶², A. Ene⁴³,
 J. Eschle⁶⁹, S. Esen²², T. Evans⁶³, F. Fabiano^{32,m}, L. N. Falcao², Y. Fan⁷, B. Fang⁷, L. Fantini^{34,49,q},
 M. Faria⁵⁰, K. Farmer⁵⁹, D. Fazzini^{31,c}, L. Felkowski⁸⁰, M. Feng^{5,7}, M. Feo¹⁹, A. Fernandez Casani⁴⁸,
 M. Fernandez Gomez⁴⁷, A. D. Fernez⁶⁷, F. Ferrari^{25,i}, F. Ferreira Rodrigues³, M. Ferrillo⁵¹, M. Ferro-Luzzi⁴⁹,
 S. Filippov⁴⁴, R. A. Fini²⁴, M. Fiorini^{26,f}, M. Firlej⁴⁰, K. L. Fischer⁶⁴, D. S. Fitzgerald⁸³, C. Fitzpatrick⁶³,
 T. Fiutowski⁴⁰, F. Fleuret¹⁵, M. Fontana²⁵, L. F. Foreman⁶³, R. Forty⁴⁹, D. Foulds-Holt⁵⁶, V. Franco Lima³,
 M. Franco Sevilla⁶⁷, M. Frank⁴⁹, E. Franzoso^{26,f}, G. Frau⁶³, C. Frei⁴⁹, D. A. Friday⁶³, J. Fu⁷, Q. Führing^{19,56,b},
 Y. Fujii¹, T. Fulghesu¹⁶, E. Gabriel³⁸, G. Galati²⁴, M. D. Galati³⁸, A. Gallas Torreira⁴⁷, D. Galli^{25,i},
 S. Gambetta⁵⁹, M. Gandelman³, P. Gandini³⁰, B. Ganie⁶³, H. Gao⁷, R. Gao⁶⁴, T. Q. Gao⁵⁶, Y. Gao⁸, Y. Gao⁶,
 Y. Gao⁸, L. M. Garcia Martin⁵⁰, P. Garcia Moreno⁴⁶, J. García Pardiñas⁴⁹, P. Gardner⁶⁷, K. G. Garg⁸,
 L. Garrido⁴⁶, C. Gaspar⁴⁹, R. E. Geertsema³⁸, L. L. Gerken¹⁹, E. Gersabeck⁶³, M. Gersabeck²⁰, T. Gershon⁵⁷,
 S. Ghizzo^{29,j}, Z. Ghorbanimoghaddam⁵⁵, L. Giambastiani^{33,g}, F. I. Giasemis^{16,r}, V. Gibson⁵⁶, H. K. Giemza⁴²,
 A. L. Gilman⁶⁴, M. Giovannetti²⁸, A. Gioventù⁴⁶, L. Girardey^{63,58}, P. Gironella Gironell⁴⁶, C. Giugliano^{26,f},
 M. A. Giza⁴¹, E. L. Gkougkousis⁶², F. C. Glaser^{14,22}, V. V. Gligorov^{16,49}, C. Göbel⁷⁰, E. Golobardes⁴⁵,
 D. Golubkov⁴⁴, A. Golutvin^{62,49,44}, S. Gomez Fernandez⁴⁶, W. Gomulka⁴⁰, F. Goncalves Abrantes⁶⁴, M. Goncerz⁴¹,
 G. Gong^{4,p}, J. A. Gooding¹⁹, I. V. Gorelov⁴⁴, C. Gotti³¹, J. P. Grabowski¹⁸, L. A. Granado Cardoso⁴⁹,
 E. Graugés⁴⁶, E. Graverini^{50,s}, L. Grazette⁵⁷, G. Graziani¹⁰, A. T. Grecu⁴³, L. M. Greeven³⁸, N. A. Grieser⁶⁶

- 590 L. Grillo⁶⁰ S. Gromov⁴⁴ C. Gu¹⁵ M. Guarise²⁶ L. Guerry¹¹ M. Guittiere¹⁴ V. Guliaeva⁴⁴ P. A. Günther²²
591 A.-K. Guseinov⁵⁰ E. Gushchin⁴⁴ Y. Guz^{6,49,44} T. Gys⁴⁹ K. Habermann¹⁸ T. Hadavizadeh¹
592 C. Hadjivasiliou⁶⁷ G. Haefeli⁵⁰ C. Haen⁴⁹ M. Hajheidari⁴⁹ G. Hallett⁵⁷ M. M. Halvorsen⁴⁹ P. M. Hamilton⁶⁷
593 J. Hammerich⁶¹ Q. Han⁸ X. Han^{22,49} S. Hansmann-Menzemer²² L. Hao⁷ N. Harnew⁶⁴ T. H. Harris¹
594 M. Hartmann¹⁴ S. Hashmi⁴⁰ J. He^{7,t} F. Hemmer⁴⁹ C. Henderson⁶⁶ R. D. L. Henderson^{1,57}
595 A. M. Hennequin⁴⁹ K. Hennessy⁶¹ L. Henry⁵⁰ J. Herd⁶² P. Herrero Gascon²² J. Heuel¹⁷ A. Hicheur³
596 G. Hijano Mendizabal⁵¹ J. Horswill⁶³ R. Hou⁸ Y. Hou¹¹ N. Howarth⁶¹ J. Hu⁷² W. Hu⁶ X. Hu^{4,p}
597 W. Huang⁷ W. Hulsbergen³⁸ R. J. Hunter⁵⁷ M. Hushchyn⁴⁴ D. Hutchcroft⁶¹ M. Idzik⁴⁰ D. Ilin⁴⁴ P. Ilten⁶⁶
598 A. Inglessi⁴⁴ A. Iniuksin⁴⁴ A. Ishteev⁴⁴ K. Ivshin⁴⁴ R. Jacobsson⁴⁹ H. Jage¹⁷ S. J. Jaimes Elles^{75,49,48}
599 S. Jakobsen⁴⁹ E. Jans³⁸ B. K. Jashal⁴⁸ A. Jawahery^{67,49} V. Jevtic^{19,b} E. Jiang⁶⁷ X. Jiang^{5,7} Y. Jiang⁷
600 Y. J. Jiang⁶ M. John⁶⁴ A. John Rubesh Rajan²³ D. Johnson⁵⁴ C. R. Jones⁵⁶ T. P. Jones⁵⁷ S. Joshi⁴²
601 B. Jost⁴⁹ J. Juan Castella⁵⁶ N. Jurik⁴⁹ I. Juszczak⁴¹ D. Kaminaris⁵⁰ S. Kandybei⁵² M. Kane⁵⁹ Y. Kang^{4,p}
602 C. Kar¹¹ M. Karacson⁴⁹ D. Karpenkov⁴⁴ A. Kauniskangas⁵⁰ J. W. Kautz⁶⁶ M. K. Kazanecki⁴¹ F. Keizer⁴⁹
603 M. Kenzie⁵⁶ T. Ketel³⁸ B. Khanji⁶⁹ A. Kharisova⁴⁴ S. Kholodenko^{35,49} G. Khreich¹⁴ T. Kirn¹⁷
604 V. S. Kirsebom^{31,c} O. Kitouni⁶⁵ S. Klaver³⁹ N. Kleijne^{35,e} K. Klimaszewski⁴² M. R. Kmiec⁴² S. Koliiev⁵³
605 L. Kolk¹⁹ A. Konoplyannikov⁴⁴ P. Kopciewicz^{40,49} P. Koppenburg³⁸ M. Korolev⁴⁴ I. Kostiuk³⁸ O. Kot⁵³
606 S. Kotriakhova⁴⁴ A. Kozachuk⁴⁴ P. Kravchenko⁴⁴ L. Kravchuk⁴⁴ M. Kreps⁵⁷ P. Krokovny⁴⁴ W. Krupa⁶⁹
607 W. Krzemien⁴² O. Kshyvanskyi⁵³ S. Kubis⁸⁰ M. Kucharczyk⁴¹ V. Kudryavtsev⁴⁴ E. Kulikova⁴⁴ A. Kupsc⁸²
608 B. K. Kutsenko¹³ D. Lacarrere⁴⁹ P. Laguarta Gonzalez⁴⁶ A. Lai³² A. Lampis³² D. Lancierini⁵⁶
609 C. Landesa Gomez⁴⁷ J. J. Lane¹ R. Lane⁵⁵ G. Lanfranchi²⁸ C. Langenbruch²² J. Langer¹⁹ O. Lantwin⁴⁴
610 T. Latham⁵⁷ F. Lazzari^{35,s} C. Lazzeroni⁵⁴ R. Le Gac¹³ H. Lee⁶¹ R. Lefèvre¹¹ A. Leflat⁴⁴ S. Legotin⁴⁴
611 M. Lehuraux⁵⁷ E. Lemos Cid⁴⁹ O. Leroy¹³ T. Lesiak⁴¹ E. D. Lesser⁴⁹ B. Leverington²² A. Li^{4,p} C. Li¹³
612 H. Li⁷² K. Li⁸ L. Li⁶³ M. Li⁸ P. Li⁷ P.-R. Li⁷³ Q. Li^{5,7} S. Li⁸ T. Li^{5,u} T. Li⁷² Y. Li⁸ Y. Li⁵
613 Z. Lian^{4,p} X. Liang⁶⁹ S. Libralon⁴⁸ C. Lin⁷ T. Lin⁵⁸ R. Lindner⁴⁹ H. Linton⁶² V. Lisovskyi⁵⁰
614 R. Litvinov^{32,49} F. L. Liu¹ G. Liu⁷² K. Liu⁷³ S. Liu^{5,7} W. Liu⁸ Y. Liu⁵⁹ Y. Liu⁷³ Y. L. Liu⁶²
615 A. Lobo Salvia⁴⁶ A. Loi³² T. Long⁵⁶ J. H. Lopes³ A. Lopez Huertas⁴⁶ S. López Soliño⁴⁷ Q. Lu¹⁵
616 C. Lucarelli²⁷ D. Lucchesi^{33,g} M. Lucio Martinez⁷⁹ V. Lukashenko^{38,53} Y. Luo⁶ A. Lupato^{33,v} E. Luppi^{26,f}
617 K. Lynch²³ X.-R. Lyu⁷ G. M. Ma^{4,p} S. Maccolini¹⁹ F. Machefert¹⁴ F. Maciuc⁴³ B. Mack⁶⁹ I. Mackay⁶⁴
618 L. M. Mackey⁶⁹ L. R. Madhan Mohan⁵⁶ M. J. Madurai⁵⁴ A. Maevskiy⁴⁴ D. Magdalinski³⁸ D. Maisuzenko⁴⁴
619 M. W. Majewski⁴⁰ J. J. Malczewski⁴¹ S. Malde⁶⁴ L. Malentacca⁴⁹ A. Malinin⁴⁴ T. Maltsev⁴⁴ G. Manca^{32,m}
620 G. Mancinelli¹³ C. Mancuso^{30,14,k} R. Manera Escalero⁴⁶ F. M. Manganella³⁷ D. Manuzzi²⁵ D. Marangotto^{30,k}
621 J. F. Marchand¹⁰ R. Marchevski⁵⁰ U. Marconi²⁵ E. Mariani¹⁶ S. Mariani⁴⁹ C. Marin Benito^{46,49} J. Marks²²
622 A. M. Marshall⁵⁵ L. Martel⁶⁴ G. Martelli^{34,q} G. Martellotti³⁶ L. Martinazzoli⁴⁹ M. Martinelli^{31,c}
623 D. Martinez Gomez⁷⁸ D. Martinez Santos⁸¹ F. Martinez Vidal⁴⁸ A. Martorell i Granollers⁴⁵ A. Massafferri²
624 R. Matev⁴⁹ A. Mathad⁴⁹ V. Matiunin⁴⁴ C. Matteuzzi⁶⁹ K. R. Mattioli¹⁵ A. Mauri⁶² E. Maurice¹⁵
625 J. Mauricio⁴⁶ P. Mayencourt⁵⁰ J. Mazorra de Cos⁴⁸ M. Mazurek⁴² M. McCann⁶² L. Mcconnell²³
626 T. H. McGrath⁶³ N. T. McHugh⁶⁰ A. McNab⁶³ R. McNulty²³ B. Meadows⁶⁶ G. Meier¹⁹ D. Melnychuk⁴²
627 F. M. Meng^{4,p} M. Merk⁵⁰ A. Merli⁵⁰ L. Meyer Garcia⁶⁷ D. Miao^{5,7} H. Miao⁷ M. Mikhasenko⁷⁶
628 D. A. Milanes⁷⁵ A. Minotti^{31,c} E. Minucci²⁸ T. Miralles¹¹ B. Mitreska¹⁹ D. S. Mitzel¹⁹ A. Modak⁵⁸
629 R. A. Mohammed⁶⁴ R. D. Moise¹⁷ S. Mokhnenko⁴⁴ E. F. Molina Cardenas⁸³ T. Mombächer⁴⁹ M. Monk^{57,1}
630 S. Monteil¹¹ A. Morcillo Gomez⁴⁷ G. Morello²⁸ M. J. Morello^{35,e} M. P. Morgenthaler²² J. Moron⁴⁰
631 W. Morren³⁸ A. B. Morris⁴⁹ A. G. Morris¹³ R. Mountain⁶⁹ H. Mu^{4,p} Z. M. Mu⁶ E. Muhammad⁵⁷
632 F. Muheim⁵⁹ M. Mulder⁷⁸ K. Müller⁵¹ F. Muñoz-Rojas⁹ R. Murta⁶² P. Naik⁶¹ T. Nakada⁵⁰
633 R. Nandakumar⁵⁸ T. Nanut⁴⁹ I. Nasteva³ M. Needham⁵⁹ N. Neri^{30,k} S. Neubert¹⁸ N. Neufeld⁴⁹
634 P. Neustroev⁴⁴ J. Nicolini^{19,14} D. Nicotra⁷⁹ E. M. Niel⁴⁹ N. Nikitin⁴⁴ Q. Niu⁷³ P. Nogarolli³ P. Nogga¹⁸
635 C. Normand⁵⁵ J. Novoa Fernandez⁴⁷ G. Nowak⁶⁶ C. Nunez⁸³ H. N. Nur⁶⁰ A. Oblakowska-Mucha⁴⁰
636 V. Obraztsov⁴⁴ T. Oeser¹⁷ S. Okamura^{26,f} A. Okhotnikov⁴⁴ O. Okhrimenko⁵³ R. Oldeman^{32,m} F. Oliva⁵⁹
637 M. Olocco¹⁹ C. J. G. Onderwater⁷⁹ R. H. O'Neil⁵⁹ D. Osthus¹⁹ J. M. Otalora Goicochea³ P. Owen⁵¹
638 A. Oyanguren⁴⁸ O. Ozcelik⁵⁹ F. Paciolla^{35,w} A. Padde⁴² K. O. Padeken¹⁸ B. Pagare⁵⁷ P. R. Pais²²

- 639 T. Pajero⁴⁹ A. Palano²⁴ M. Palutan²⁸ X. Pan^{4,p} G. Panshin⁴⁴ L. Paolucci⁵⁷ A. Papanestis^{58,49}
 640 M. Pappagallo^{24,o} L. L. Pappalardo^{26,f} C. Pappenheimer⁶⁶ C. Parkes⁶³ D. Parmar⁷⁶ B. Passalacqua^{26,f}
 641 G. Passaleva²⁷ D. Passaro^{35,e} A. Pastore²⁴ M. Patel⁶² J. Patoc⁶⁴ C. Patrignani^{25,i} A. Paul⁶⁹ C. J. Pawley⁷⁹
 642 A. Pellegrino³⁸ J. Peng^{5,7} M. Pepe Altarelli²⁸ S. Perazzini²⁵ D. Pereima⁴⁴ H. Pereira Da Costa⁶⁸
 643 A. Pereiro Castro⁴⁷ P. Perret¹¹ A. Perrevoort⁷⁸ A. Perro^{49,13} M. J. Peters⁶⁶ K. Petridis⁵⁵ A. Petrolini^{29,j}
 644 J. P. Pfaller⁶⁶ H. Pham⁶⁹ L. Pica^{35,e} M. Piccini³⁴ L. Piccolo³² B. Pietrzyk¹⁰ G. Pietrzyk¹⁴ D. Pinci³⁶
 645 F. Pisani⁴⁹ M. Pizzichemi^{31,49,c} V. Placinta⁴³ M. Plo Casasus⁴⁷ T. Poeschl⁴⁹ F. Polci^{16,49} M. Poli Lener²⁸
 646 A. Poluektov¹³ N. Polukhina⁴⁴ I. Polyakov⁴⁴ E. Polycarpo³ S. Ponce⁴⁹ D. Popov⁷ S. Poslavskii⁴⁴
 647 K. Prasanth⁵⁹ C. Prouve⁸¹ D. Provenzano^{32,m} V. Pugatch⁵³ G. Punzi^{35,s} S. Qasim⁵¹ Q. Q. Qian⁶ W. Qian⁷
 648 N. Qin^{4,p} S. Qu^{4,p} R. Quagliani⁴⁹ R. I. Rabadan Trejo⁵⁷ J. H. Rademacker⁵⁵ M. Rama³⁵
 649 M. Ramírez García⁸³ V. Ramos De Oliveira⁷⁰ M. Ramos Pernas⁵⁷ M. S. Rangel³ F. Ratnikov⁴⁴ G. Raven³⁹
 650 M. Rebollo De Miguel⁴⁸ F. Redi^{30,v} J. Reich⁵⁵ F. Reiss⁶³ Z. Ren⁷ P. K. Resmi⁶⁴ R. Ribatti⁵⁰
 651 G. R. Ricart^{15,12} D. Riccardi^{35,e} S. Ricciardi⁵⁸ K. Richardson⁶⁵ M. Richardson-Slipper⁵⁹ K. Rinnert⁶¹
 652 P. Robbe^{14,49} G. Robertson⁶⁰ E. Rodrigues⁶¹ A. Rodriguez Alvarez⁴⁶ E. Rodriguez Fernandez⁴⁷
 653 J. A. Rodriguez Lopez⁷⁵ E. Rodriguez Rodriguez⁴⁷ J. Roensch¹⁹ A. Rogachev⁴⁴ A. Rogovskiy⁵⁸ D. L. Rolf⁴⁹
 654 P. Roloff⁴⁹ V. Romanovskiy⁶⁶ A. Romero Vidal⁴⁷ G. Romolini²⁶ F. Ronchetti⁵⁰ T. Rong⁶ M. Rotondo²⁸
 655 S. R. Roy²² M. S. Rudolph⁶⁹ M. Ruiz Diaz²² R. A. Ruiz Fernandez⁴⁷ J. Ruiz Vidal^{82,x} A. Ryzhikov⁴⁴
 656 J. Ryzka⁴⁰ J. J. Saavedra-Arias⁹ J. J. Saborido Silva⁴⁷ R. Sadek¹⁵ N. Sagidova⁴⁴ D. Sahoo⁷⁷ N. Sahoo⁵⁴
 657 B. Saitta^{32,m} M. Salomoni^{31,49,c} I. Sanderswood⁴⁸ R. Santacesaria³⁶ C. Santamarina Rios⁴⁷ M. Santimaria^{28,49}
 658 L. Santoro² E. Santovetti³⁷ A. Saputi^{26,49} D. Saranin⁴⁴ A. Sarnatskiy⁷⁸ G. Sarpis⁵⁹ M. Sarpis⁶³
 659 C. Satriano^{36,y} A. Satta³⁷ M. Saur⁶ D. Savrina⁴⁴ H. Sazak¹⁷ F. Sborzacchi^{49,28} L. G. Scantlebury Smead⁶⁴
 660 A. Scarabotto¹⁹ S. Schael¹⁷ S. Scherl⁶¹ M. Schiller⁶⁰ H. Schindler⁴⁹ M. Schmelling²¹ B. Schmidt⁴⁹
 661 S. Schmitt¹⁷ H. Schmitz¹⁸ O. Schneider⁵⁰ A. Schopper⁴⁹ N. Schulte¹⁹ S. Schulte⁵⁰ M. H. Schune¹⁴
 662 R. Schwemmer⁴⁹ G. Schwering¹⁷ B. Sciascia²⁸ A. Sciuccati⁴⁹ I. Segal⁷⁶ S. Sellam⁴⁷ A. Semennikov⁴⁴
 663 T. Senger⁵¹ M. Senghi Soares³⁹ A. Sergi^{29,j} N. Serra⁵¹ L. Sestini³³ A. Seuthe¹⁹ Y. Shang⁶
 664 D. M. Shangase⁸³ M. Shapkin⁴⁴ R. S. Sharma⁶⁹ I. Shchemberov⁴⁴ L. Shchutska⁵⁰ T. Shears⁶¹
 665 L. Shekhtman⁴⁴ Z. Shen⁶ S. Sheng^{5,7} V. Shevchenko⁴⁴ B. Shi⁷ Q. Shi⁷ Y. Shimizu¹⁴ E. Shmanin²⁵
 666 R. Shorkin⁴⁴ J. D. Shupperd⁶⁹ R. Silva Coutinho⁶⁹ G. Simi^{33,g} S. Simone^{24,o} N. Skidmore⁵⁷
 667 T. Skwarnicki⁶⁹ M. W. Slater⁵⁴ J. C. Smallwood⁶⁴ E. Smith⁶⁵ K. Smith⁶⁸ M. Smith⁶² A. Snoch³⁸
 668 L. Soares Lavra⁵⁹ M. D. Sokoloff⁶⁶ F. J. P. Soler⁶⁰ A. Solomin^{44,55} A. Solovev⁴⁴ I. Solovyev⁴⁴
 669 N. S. Sommerfeld¹⁸ R. Song¹ Y. Song⁵⁰ Y. Song^{4,p} Y. S. Song⁶ F. L. Souza De Almeida⁶⁹
 670 B. Souza De Paula³ E. Spadaro Norella^{29,j} E. Spedicato²⁵ J. G. Speer¹⁹ E. Spiridenkov⁴⁴ P. Spradlin⁶⁰
 671 V. Sriskaran⁴⁹ F. Stagni⁴⁹ M. Stahl⁴⁹ S. Stahl⁴⁹ S. Stanislaus⁶⁴ E. N. Stein⁴⁹ O. Steinkamp⁵¹ O. Stenyakin⁴⁴
 672 H. Stevens¹⁹ D. Strekalina⁴⁴ Y. Su⁷ F. Suljik⁶⁴ J. Sun³² L. Sun⁷⁴ D. Sundfeld² W. Sutcliffe⁵¹
 673 P. N. Swallow⁵⁴ K. Swientek⁴⁰ F. Swystun⁵⁶ A. Szabelski⁴² T. Szumlak⁴⁰ Y. Tan^{4,p} Y. Tang⁷⁴ M. D. Tat⁶⁴
 674 A. Terentev⁴⁴ F. Terzuoli^{35,49,w} F. Teubert⁴⁹ E. Thomas⁴⁹ D. J. D. Thompson⁵⁴ H. Tilquin⁶² V. Tisserand¹¹
 675 S. T'Jampens¹⁰ M. Tobin^{5,49} L. Tomassetti^{26,f} G. Tonani^{30,49,k} X. Tong⁶ D. Torres Machado² L. Toscano¹⁹
 676 D. Y. Tou^{4,p} C. Trippel⁴⁵ G. Tuci²² N. Tuning³⁸ L. H. Uecker²² A. Ukleja⁴⁰ D. J. Unverzagt²² B. Urbach⁵⁹
 677 E. Ursov⁴⁴ A. Usachov³⁹ A. Ustyuzhanin⁴⁴ U. Uwer²² V. Vagnoni²⁵ V. Valcarce Cadenas⁴⁷ G. Valenti²⁵
 678 N. Valls Canudas⁴⁹ J. van Eldik⁴⁹ H. Van Hecke⁶⁸ E. van Herwijnen⁶² C. B. Van Hulse^{47,z} R. Van Laak⁵⁰
 679 M. van Veghel³⁸ G. Vasquez⁵¹ R. Vazquez Gomez⁴⁶ P. Vazquez Regueiro⁴⁷ C. Vázquez Sierra⁴⁷ S. Vecchi²⁶
 680 J. J. Velthuis⁵⁵ M. Veltri^{27,aa} A. Venkateswaran⁵⁰ M. Verdoglia³² M. Vesterinen⁵⁷ D. Vico Benet⁶⁴
 681 P. Vidrier Villalba⁴⁶ M. Vieites Diaz⁴⁹ X. Vilasis-Cardona⁴⁵ E. Vilella Figueras⁶¹ A. Villa²⁵ P. Vincent¹⁶
 682 F. C. Volle⁵⁴ D. vom Bruch¹³ N. Voropaev⁴⁴ K. Vos⁷⁹ C. Vrahatis⁵⁹ J. Wagner¹⁹ J. Walsh³⁵ E. J. Walton^{1,57}
 683 G. Wan⁶ C. Wang²² G. Wang⁸ H. Wang⁷³ J. Wang⁶ J. Wang⁵ J. Wang^{4,p} J. Wang⁷⁴ M. Wang³⁰
 684 N. W. Wang⁷ R. Wang⁵⁵ X. Wang⁸ X. Wang⁷² X. W. Wang⁶² Y. Wang⁶ Y. W. Wang⁷³ Z. Wang¹⁴
 685 Z. Wang^{4,p} Z. Wang³⁰ J. A. Ward^{57,1} M. Waterlaat⁴⁹ N. K. Watson⁵⁴ D. Websdale⁶² Y. Wei⁶ J. Wendel⁸¹
 686 B. D. C. Westhenry⁵⁵ C. White⁵⁶ M. Whitehead⁶⁰ E. Whiter⁵⁴ A. R. Wiederhold⁶³ D. Wiedner¹⁹
 687 G. Wilkinson⁶⁴ M. K. Wilkinson⁶⁶ M. Williams⁶⁵ M. J. Williams⁴⁹ M. R. J. Williams⁵⁹ R. Williams⁵⁶

Z. Williams⁵⁵, F. F. Wilson⁵⁸, M. Winn¹², W. Wislicki⁴², M. Witek⁴¹, L. Witola²², G. Wormser¹⁴, S. A. Wotton⁵⁶, H. Wu⁶⁹, J. Wu⁸, X. Wu⁷⁴, Y. Wu⁶, Z. Wu⁷, K. Wyllie⁴⁹, S. Xian⁷², Z. Xiang⁵, Y. Xie⁸, A. Xu³⁵, J. Xu⁷, L. Xu^{4,p}, L. Xu^{4,p}, M. Xu⁵⁷, Z. Xu⁴⁹, Z. Xu⁷, Z. Xu⁵, K. Yang⁶², S. Yang⁷, X. Yang⁶, Y. Yang^{29,j}, Z. Yang⁶, V. Yeroshenko¹⁴, H. Yeung⁶³, H. Yin⁸, X. Yin⁷, C. Y. Yu⁶, J. Yu⁷¹, X. Yuan⁵, Y. Yuan^{5,7}, E. Zaffaroni⁵⁰, M. Zavertyaev²¹, M. Zdybal⁴¹, F. Zenesini^{25,i}, C. Zeng^{5,7}, M. Zeng^{4,p}, C. Zhang⁶, D. Zhang⁸, J. Zhang⁷, L. Zhang^{4,p}, S. Zhang⁷¹, S. Zhang⁶⁴, Y. Zhang⁶, Y. Z. Zhang^{4,p}, Z. Zhang^{4,p}, Y. Zhao²², A. Zharkova⁴⁴, A. Zhelezov²², S. Z. Zheng⁶, X. Z. Zheng^{4,p}, Y. Zheng⁷, T. Zhou⁶, X. Zhou⁸, Y. Zhou⁷, V. Zhovkovska⁵⁷, L. Z. Zhu⁷, X. Zhu^{4,p}, X. Zhu⁸, V. Zhukov¹⁷, J. Zhuo⁴⁸, Q. Zou^{5,7}, D. Zuliani^{33,g}, and G. Zunica⁵⁰

(LHCb Collaboration)

¹School of Physics and Astronomy, Monash University, Melbourne, Australia²Centro Brasileiro de Pesquisas Físicas (CBPF), Rio de Janeiro, Brazil³Universidade Federal do Rio de Janeiro (UFRJ), Rio de Janeiro, Brazil⁴Department of Engineering Physics, Tsinghua University, Beijing, China⁵Institute Of High Energy Physics (IHEP), Beijing, China⁶School of Physics State Key Laboratory of Nuclear Physics and Technology, Peking University, Beijing, China⁷University of Chinese Academy of Sciences, Beijing, China⁸Institute of Particle Physics, Central China Normal University, Wuhan, Hubei, China⁹Consejo Nacional de Rectores (CONARE), San Jose, Costa Rica¹⁰Université Savoie Mont Blanc, CNRS, IN2P3-LAPP, Annecy, France¹¹Université Clermont Auvergne, CNRS/IN2P3, LPC, Clermont-Ferrand, France¹²Université Paris-Saclay, Centre d'Etudes de Saclay (CEA), IRFU, Saclay, France, Gif-Sur-Yvette, France¹³Aix Marseille Univ, CNRS/IN2P3, CPPM, Marseille, France¹⁴Université Paris-Saclay, CNRS/IN2P3, IJCLab, Orsay, France¹⁵Laboratoire Leprince-Ringuet, CNRS/IN2P3, Ecole Polytechnique, Institut Polytechnique de Paris, Palaiseau, France¹⁶LPNHE, Sorbonne Université, Paris Diderot Sorbonne Paris Cité, CNRS/IN2P3, Paris, France¹⁷I. Physikalisches Institut, RWTH Aachen University, Aachen, Germany¹⁸Universität Bonn - Helmholtz-Institut für Strahlen und Kernphysik, Bonn, Germany¹⁹Fakultät Physik, Technische Universität Dortmund, Dortmund, Germany²⁰Physikalischs Institut, Albert-Ludwigs-Universität Freiburg, Freiburg, Germany²¹Max-Planck-Institut für Kernphysik (MPIK), Heidelberg, Germany²²Physikalischs Institut, Ruprecht-Karls-Universität Heidelberg, Heidelberg, Germany²³School of Physics, University College Dublin, Dublin, Ireland²⁴INFN Sezione di Bari, Bari, Italy²⁵INFN Sezione di Bologna, Bologna, Italy²⁶INFN Sezione di Ferrara, Ferrara, Italy²⁷INFN Sezione di Firenze, Firenze, Italy²⁸INFN Laboratori Nazionali di Frascati, Frascati, Italy²⁹INFN Sezione di Genova, Genova, Italy³⁰INFN Sezione di Milano, Milano, Italy³¹INFN Sezione di Milano-Bicocca, Milano, Italy³²INFN Sezione di Cagliari, Monserrato, Italy³³INFN Sezione di Padova, Padova, Italy³⁴INFN Sezione di Perugia, Perugia, Italy³⁵INFN Sezione di Pisa, Pisa, Italy³⁶INFN Sezione di Roma La Sapienza, Roma, Italy³⁷INFN Sezione di Roma Tor Vergata, Roma, Italy³⁸Nikhef National Institute for Subatomic Physics, Amsterdam, Netherlands³⁹Nikhef National Institute for Subatomic Physics and VU University Amsterdam, Amsterdam, Netherlands⁴⁰AGH - University of Krakow, Faculty of Physics and Applied Computer Science, Kraków, Poland⁴¹Henryk Niewodniczanski Institute of Nuclear Physics Polish Academy of Sciences, Kraków, Poland⁴²National Center for Nuclear Research (NCBJ), Warsaw, Poland⁴³Horia Hulubei National Institute of Physics and Nuclear Engineering, Bucharest-Magurele, Romania⁴⁴Authors affiliated with an institute formerly covered by a cooperation agreement with CERN

- 44 ⁴⁵*DS4DS, La Salle, Universitat Ramon Llull, Barcelona, Spain*
 45 ⁴⁶*ICCUB, Universitat de Barcelona, Barcelona, Spain*
 46 ⁴⁷*Instituto Galego de Física de Altas Enerxías (IGFAE), Universidade de Santiago de Compostela, Santiago de Compostela, Spain*
 47 ⁴⁸*Instituto de Física Corpuscular, Centro Mixto Universidad de Valencia - CSIC, Valencia, Spain*
 48 ⁴⁹*European Organization for Nuclear Research (CERN), Geneva, Switzerland*
 49 ⁵⁰*Institute of Physics, Ecole Polytechnique Fédérale de Lausanne (EPFL), Lausanne, Switzerland*
 50 ⁵¹*Physik-Institut, Universität Zürich, Zürich, Switzerland*
 51 ⁵²*NSC Kharkiv Institute of Physics and Technology (NSC KIPT), Kharkiv, Ukraine*
 52 ⁵³*Institute for Nuclear Research of the National Academy of Sciences (KINR), Kyiv, Ukraine*
 53 ⁵⁴*School of Physics and Astronomy, University of Birmingham, Birmingham, United Kingdom*
 54 ⁵⁵*H.H. Wills Physics Laboratory, University of Bristol, Bristol, United Kingdom*
 55 ⁵⁶*Cavendish Laboratory, University of Cambridge, Cambridge, United Kingdom*
 56 ⁵⁷*Department of Physics, University of Warwick, Coventry, United Kingdom*
 57 ⁵⁸*STFC Rutherford Appleton Laboratory, Didcot, United Kingdom*
 58 ⁵⁹*School of Physics and Astronomy, University of Edinburgh, Edinburgh, United Kingdom*
 59 ⁶⁰*School of Physics and Astronomy, University of Glasgow, Glasgow, United Kingdom*
 60 ⁶¹*Oliver Lodge Laboratory, University of Liverpool, Liverpool, United Kingdom*
 61 ⁶²*Imperial College London, London, United Kingdom*
 62 ⁶³*Department of Physics and Astronomy, University of Manchester, Manchester, United Kingdom*
 63 ⁶⁴*Department of Physics, University of Oxford, Oxford, United Kingdom*
 64 ⁶⁵*Massachusetts Institute of Technology, Cambridge, Massachusetts, USA*
 65 ⁶⁶*University of Cincinnati, Cincinnati, Ohio, USA*
 66 ⁶⁷*University of Maryland, College Park, Maryland, USA*
 67 ⁶⁸*Los Alamos National Laboratory (LANL), Los Alamos, New Mexico, USA*
 68 ⁶⁹*Syracuse University, Syracuse, New York, USA*
 69 ⁷⁰*Pontifícia Universidade Católica do Rio de Janeiro (PUC-Rio), Rio de Janeiro, Brazil*
 70 *(associated with Universidade Federal do Rio de Janeiro (UFRJ), Rio de Janeiro, Brazil)*
 71 ⁷²*School of Physics and Electronics, Hunan University, Changsha City, China*
 72 *(associated with Institute of Particle Physics, Central China Normal University, Wuhan, Hubei, China)*
 73 ⁷⁴*Guangdong Provincial Key Laboratory of Nuclear Science, Guangdong-Hong Kong Joint Laboratory of Quantum Matter, Institute of Quantum Matter, South China Normal University, Guangzhou, China*
 74 *(associated with Department of Engineering Physics, Tsinghua University, Beijing, China)*
 75 ⁷⁶*Lanzhou University, Lanzhou, China*
 76 *(associated with Institute Of High Energy Physics (IHEP), Beijing, China)*
 77 ⁷⁸*School of Physics and Technology, Wuhan University, Wuhan, China*
 78 *(associated with Department of Engineering Physics, Tsinghua University, Beijing, China)*
 79 ⁸⁰*Departamento de Fisica, Universidad Nacional de Colombia, Bogota, Colombia*
 80 *(associated with LPNHE, Sorbonne Université, Paris Diderot Sorbonne Paris Cité, CNRS/IN2P3, Paris, France)*
 81 ⁸²*Ruhr Universitaet Bochum, Fakultaet f. Physik und Astronomie, Bochum, Germany*
 82 *(associated with Fakultät Physik, Technische Universität Dortmund, Dortmund, Germany)*
 83 ⁸⁴*Eotvos Lorand University, Budapest, Hungary*
 84 *(associated with European Organization for Nuclear Research (CERN), Geneva, Switzerland)*
 85 ⁸⁶*Van Swinderen Institute, University of Groningen, Groningen, Netherlands*
 86 *(associated with Nikhef National Institute for Subatomic Physics, Amsterdam, Netherlands)*
 87 ⁸⁸*Universiteit Maastricht, Maastricht, Netherlands*
 88 *(associated with Nikhef National Institute for Subatomic Physics, Amsterdam, Netherlands)*
 89 ⁹⁰*Tadeusz Kosciuszko Cracow University of Technology, Cracow, Poland*
 90 *(associated with Henryk Niewodniczanski Institute of Nuclear Physics Polish Academy of Sciences, Kraków, Poland)*
 91 ⁹²*Universidade da Coruña, A Coruña, Spain*
 92 *(associated with DS4DS, La Salle, Universitat Ramon Llull, Barcelona, Spain)*
 93 ⁹⁴*Department of Physics and Astronomy, Uppsala University, Uppsala, Sweden*
 94 *(associated with School of Physics and Astronomy, University of Glasgow, Glasgow, United Kingdom)*

⁸³*University of Michigan, Ann Arbor, Michigan, USA*

(associated with Syracuse University, Syracuse, New York, USA)

^aDeceased.

^b Also at Lamarr Institute for Machine Learning and Artificial Intelligence, Dortmund, Germany.

^c Also at Università degli Studi di Milano-Bicocca, Milano, Italy.

^d Also at Università di Roma Tor Vergata, Roma, Italy.

^eAlso at Scuola Normale Superiore, Pisa, Italy.

^fAlso at Università di Ferrara, Ferrara, Italy.

^g Also at Università di Padova, Padova, Italy.

^h Also at Facultad de Ciencias Fisicas, Madrid.

ⁱAlso at Università di Bologna, Bologna, Italy.

^jAlso at Università di Genova, Genova, Italy.

^k Also at Università degli Studi di Milano, Milan.

¹Also at Universidad Nacional Autónoma de H

^mAlso at Università di Cagliari, Cagliari, Italy.

ⁿAlso at Centro Federal de Educação Tecnológica Celso Suckow da Fonseca, Rio De Janeiro, Brazil.

^oAlso at Università di Bari, Bari, Italy.

^p Also at Center for High Energy Physics, Tsinghua University, Beijing, China

^qAlso at Università di Perugia, Perugia, Italy.

^r Also at LIP6, Sorbonne Université, Paris, France.

^sAlso at Università di Pisa, Pisa, Italy.

^t Also at Hangzhou Institute for Advanced Study, UCAS, Hangzhou, China

^u Also at School of Physics and Electronics, Henan University, Kaifeng, China.

^vAlso at Università di Bergamo, Bergamo, Italy.

^wAlso at Università di Siena, Siena, Italy.

^x Also at Department of Physics/Division of Particle Physics, Lund, Sweden.

^yAlso at Università della Basilicata, Potenza, Italy

^z Also at Universidad de Alcalá, Alcalá de Henares.

^{aa} Also at Università di Urbino, Urbino, Italy

Also at Università di Urbino, Urbino, Italy.